Atmospheric Oxidation Mechanism of Hydroxymethyl Hydroperoxide†

Joseph S. Francisco*,‡ and Wolfgang Eisfeld*,§

Department of Chemistry and Department of Earth & Atmospheric Sciences, Purdue University, West Lafayette, Indiana 47907-2084, Theoretische Chemie, Fakultät für Chemie, Universität Bielefeld, Postfach 100131, D-33501 Bielefeld, Germany

Received: February 25, 2009; Revised Manuscript Received: April 30, 2009

A mechanism for the atmospheric oxidation of hydroxymethyl hydroperoxide (HMHP) by hydroxyl radicals (OH) is proposed from an ab initio study. Using CCSD(T)/6-311++G(2df,2p)//MP2/6-31G(d) level of theory, the structures and energetics of intermediates and transition states involved in the atmospheric oxidation of HMHP are examined. Critical structures also are studied by multireference techniques (CASPT2 and MR-SDCI) to ensure the reliability of the results. From these calculations, reaction enthalpies and barrier heights are presented for three different reaction pathways for the atmospheric oxidation of HMHP. The oxidation reaction can be initiated by hydrogen abstraction at three different positions. Results suggest that the hydrogen abstraction from the carbon is the dominant pathway because this is the process with the lowest entrance barrier. This H abstraction is followed by spontaneous decomposition without any stable intermediates and leads straight to the formation of formic acid and OH radicals. Thus, an oxidative degradation of HMHP into HC(O)OH and water occurs that is catalyzed by OH radicals. These results support the suggestion that HMHP could be an atmospheric source of formic acid. The two competing but less favorable oxidation pathways may contribute to the HO_x abundance in the atmosphere. A new minor byproduct of the oxidation of HMHP predicted from the calculations is HC(O)OOH.

I. Introduction

Hydroxymethyl hydroperoxide ($HOCH_2OOH$ or HMHP), since its first observation in the atmosphere in 1989,[1] has been paid considerable scientific attention.[2−16] One reason for the significant interest in this species is that it is implicated in contributing to forest decline.[17] Although the atmospheric abundance of HMHP is not well-known, its concentration has been measured to be as high as 5 ppbv under conditions of high concentrations of ozone and isoprene. Laboratory studies have shown that the reaction of ozone with alkenes in moist air is a source of hydroxyalkyl hydroperoxide, such as hydroxymethyl hydroperoxide.[18−22]

There are a number of studies that have focused on the atmospheric fate of HMHP. Su et al.[23,24] determined photolysis rates for HMHP in UV. Bauerle and Moortgat[25] reported absorption cross sections between 205 and 360 nm. They also suggested that the photodissociation of HMHP is likely to behave similarly to other peroxides, such as HOOH and CH_3OOH, in which dissociation occurs along the O−O bond, resulting in the formation of OH and $HOCH_2O$ radicals. Interestingly, the dissociation along the C−OH bond can also produce OH radicals. Our recent study of the excited states of HMHP confirmed that excitations between 205 and 360 nm result in dissociation along the O−O bond.[26] However, the atmospheric oxidative degradation mechanism of HMHP following photodissociation is completely unknown. Studies by Fry et al.[27] examined the photodissociation of HMHP by vibrational overtone excitation. The observed product from these studies is OH radicals. Fry et al.[27] found that vibrational-overtone-induced dissocation is much slower than UV photodissociation; that is, 3.6×10^{-9} s^{-1} versus 3×10^{-6} s^{-1}. Consequently, since both optical processes are not particularly efficient, loss of HMHP in the atmosphere from removal by OH radicals is expected to be important. However, no studies of the removal of HMHP by OH radicals in the atmosphere have been reported. On the other hand, an atmospheric lifetime has been reported for HMHP on the basis of the removal of peroxides such as CH_3OOH by OH radicals.[25] The byproducts that result from the oxidation of HMHP following reaction with OH radicals are not clear, either.

In the present study, the degradation mechanism for the atmospheric oxidation of HMHP by OH radicals is examined. The goal is to determine the site at which the OH radical attacks HMHP and identify what are the probable resulting species from the atmospheric oxidation process.

II. Computational Methods

The Gaussian03 suite of programs is used to perform all the single-reference calculations described in this article.[28] CASSCF and CASPT2 calculations have been performed with the Molpro suite of programs.[29] The geometries of all the molecules considered in the oxidation pathways for HMHP are fully optimized, and their frequencies are obtained with the second-order Møller−Plesset (MP2) perturbation method.[30] All transition state structures possess one imaginary frequency. The expectation value of the total spin, $\langle S^2 \rangle$, was monitored to detect the extent of spin contamination of the system in the calculations. The largest preannihilation deviation from the expected S^2 value of 0.75 was less than 7%, and therefore, spin contamination was very small for the stationary points of the HMHP + OH atmospheric oxidation mechanism. The MP2-optimized geometries are used in a series of single-point energy calculations involving four levels of theory: PMP4/6-311++G(2d,2p), CCSD(T)/6-31++G(2d,2p), PMP4/6-311++-

† Part of the "Robert Benny Gerber Festschrift".

* Corresponding author. E-mail: eisfeld@uni-bielefeld.de.
‡ Electronic address: francisc@purdue.edu.
§ Electronic address: wolfgang.eisfeld@uni-bielefeld.de.

10.1021/jp901735z CCC: $40.75
Published on Web 05/19/2009

G2df,2p), and CCSD(T)/6-311++G(2df,2p). All of the values discussed in the following are an average of CCSD(T)/6-311++G(2df,2p)//MP2/6-31G(d) and PMP4/6-311++G(2df,2p)//MP2/6-31G(d) levels of theory unless otherwise stated. Zero-point enery (ZPE) corrections are added to the final predicted energetics. We have found that optimization of the geometries of similar chemical systems of first-row atoms at the MP2/6-31G(d) level of theory is sufficient to give good geometries that can be used with high level correlation methods and larger basis sets to get good relative energetics.[31−33] In studying the decomposition of such systems, the procedure of averaging the single point relative energies of different correlation treatments was shown to improve the estimated energetics compared to experiment.[34]

The single-reference treatment of multiple open shells coupled to less than maximum total spin is not possible. This is simply due to the fact that only the maximum or minimum possible M_s state for a given number of single spins can be represented by a single Slater determinant. For example, three unpaired electrons of $m_s = \pm 1/2$ can give $M_s = 3/2, 1/2, -1/2, -3/2$ and total spin of $S = 3/2, 1/2$. Only spin states $|S,M_s\rangle = |3/2, \pm 3/2\rangle$, thus corresponding to quartet states, are described by a single Slater determinant. All other pure spin states are linear combinations of three determinants in which the three m_s values add up to $M_s = \pm 1/2$. Such a situation may arise when triplet oxygen is reacting with a doublet radical because, in general, the lowest energy pathway is observed on the doublet potential energy surface. The potential artifacts arising from single-reference treatments of such a situation have been studied in detail before.[35] For this reason, we performed control calculations of the transition states (TS4 and TS8) corresponding to such a situation using appropriate multireference methods, particularly CASPT2. The geometries of reactants and transition states were optimized by an external optimizer, using CASPT2 energies[36] and gradients.[37] The aug-cc-pVDZ atomic basis was utilized for these calculations.[38,39] The accuracy of the energy calculations was improved by single-point calculations using the aug-cc-pVTZ atomic basis[38,39] and the internally contracted CASPT2 method.[40] Details of the active space will be given below. The most reliable energies were finally obtained by the internally contracted multiconfiguration-reference configuration interaction (MR-SDCI) method[41,42] and the aug-cc-pVTZ atomic basis. All MRCI energies are corrected for unlinked clusters by the multireference version of Davidson correction.

III. Results and Discussion

A. Reaction Pathways in the Atmospheric Degradation of HMHP. The structure of HMHP has only single bonds, and therefore, the only reasonable initial step of the degradation by OH radicals is abstraction of a hydrogen atom. However, there are three different types of hydrogens present in HMHP, opening the possibility of three different reaction pathways. There is one peroxidic hydrogen from the HOO-group on HMHP, the alcoholic hydrogen from the HO-group, and two α-carbon hydrogens.

The three different possible reaction pathways are depicted in Figure 1. Pathway 1 is initiated by hydrogen abstraction from the hydroperoxide site, resulting in a peroxy radical. Such species are usually reduced by NO (if present) and form the corresponding oxy radicals. The interesting point in the so-formed hydroxy methyloxy radical is the possibility of three different decay pathways: release of an OH radical to form formaldehyde, spontaneous release of a hydrogen atom, or H abstraction by O_2 to form formic acid.

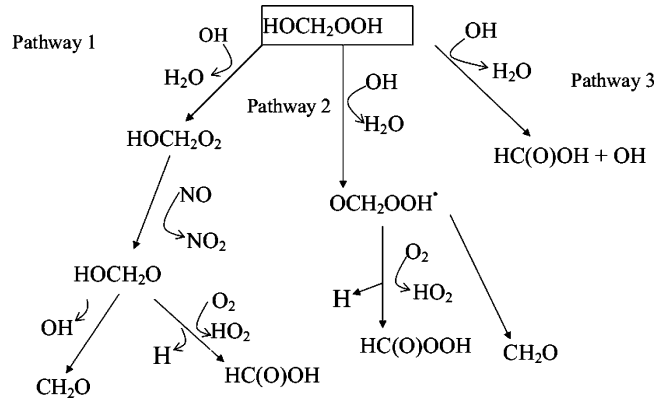

Figure 1. Atmospheric oxidation pathways of hydroxymethyl hydroperoxide (HMHP).

Pathway 2 is induced by OH abstracting the alcoholic H atom to form the so-far unknown oxy methylhydroperoxide radical. This species could deactivate itself by splitting into HO_2 and H_2CO. On the other hand, it could release a hydrogen to form the peroxy acid HC(O)OOH or this H atom is abstracted by O_2.

The third pathway is due to abstraction of an α-carbon hydrogen. The most likely fate of the formed radical is addition of O_2 to the central carbon, followed by reduction by NO. The oxy radical generated this way can be deactivated by several possibilities. Release or abstraction of the remaining α-carbon H would yield the peroxy analogon of carbonic acid, which is not very likely to be a stable species in the gas phase. Another possibility is to split into the peroxy acid and OH, thus yielding the same main product as pathway 2. Finally, the intermediate could also release HO_2 and form formic acid as in pathway 1. In the absence of NO, the formed peroxy radical might deactivate by the release of HO_2, or an oxygen molecule could abstract the hydroxylic H directly without forming the peroxy radical. As we will show below, none of these pathways is relevant, since the proposed intermediate decomposes spontaneously into formic acid and OH.

1. Structures of the Species Involved in the Atmospheric Degradation of HMHP. The initial step of pathway 1 (Figure 1) generates the $HOCH_2O_2^{\bullet}$ radical intermediate (Figure 2f). Changes in the structure of the HMHP parent molecule and the $HOCH_2O_2^{\bullet}$ radical are noticeable. The O−O bond of the radical is considerably shorter than the O−O bond in HMHP by 0.150 Å in the radical. The peroxy radical reacts with NO to form $HOCH_2O^{\bullet}$ alkoxy radical (Figure 2g). The C−O bond with the unpaired electron on the terminal oxygen is 1.364 Å long, which is consistent with the C−O bond in alkoxy radicals, such as methoxy,[43,44] and also with its isoelectronic partner, CH_2FO.[45,46] The $HOCH_2O^{\bullet}$ radical decomposes into CH_2O + OH or HC(O)OH + H$^{\bullet}$. Figure 3b shows the transition state for the formation of CH_2O + OH. In this transition state, the C−O bond decreases to 1.235 Å from 1.364 Å in the $HOCH_2O^{\bullet}$ radical, as it approaches the formation of a carbonyl C═O in CH_2O of 1.220 Å (Figure 2b). Also notice that the O−C−O angle of 91.3° of the departing OH radical is similar to the O−C−H angle of 94.6° in the departing H atom in the transition state for the formation of the HC(O)OH + H products shown in Figure 3c. An O_2 molecule can react with the $HOCH_2O$ radical to produce HC(O)OH + HO_2. The transition state for this reaction, TS4, is shown in Figure 3d. This reaction causes the attacked C−H bond to increase to 1.221 Å. The newly forming H−O bond is 1.448 Å as it makes the HO_2 radical. The approach of the oxygen of O_2 to the C−H bond of the

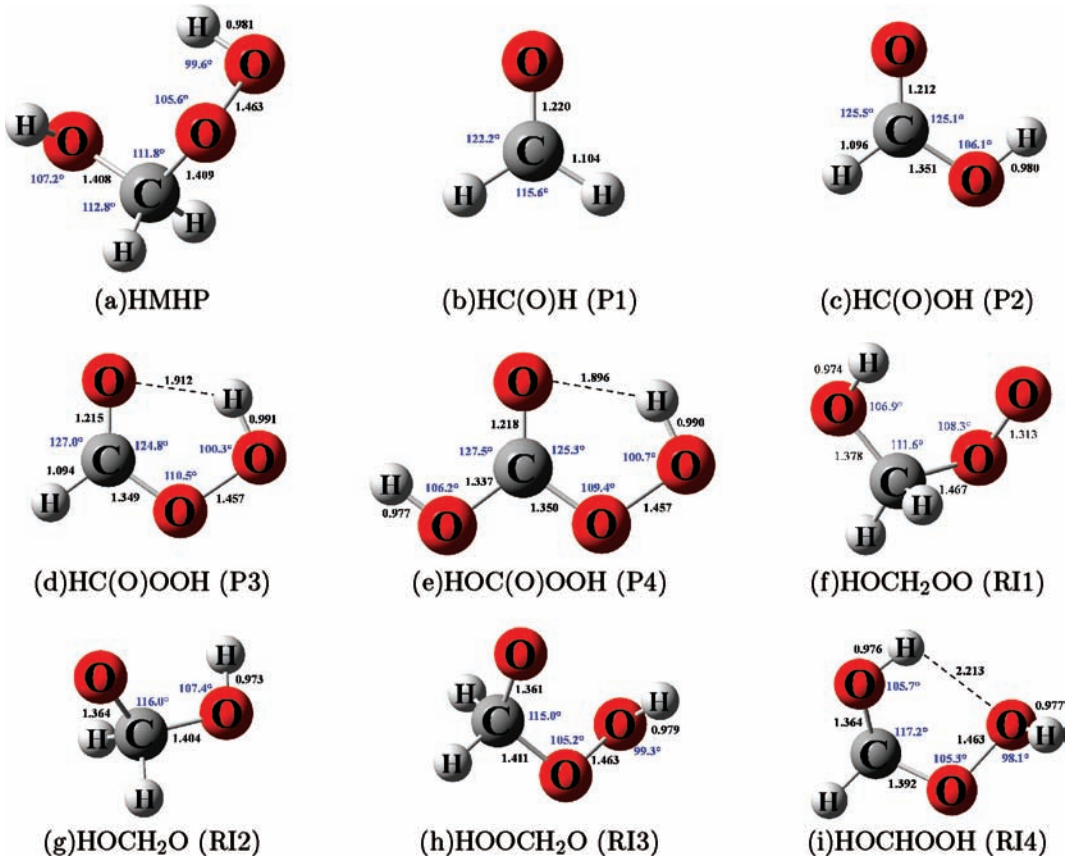

Figure 2. Structures of reactants, products (P*n*), and reaction intermediates (RI*n*) involved in the atmospheric oxidation of HMHP.

$HOCH_2O$ radical is along a slightly bent route, as shown by the C−H···O angle of 142.7° in the transition state. The short O−O distance of 2.200 Å between the O_2 fragement and the radical O atom indicates that this structure is due to an additional interaction.

As mentioned in Section II, the situation of a triplet O_2 molecule interacting with a doublet radical and spin-coupled to a doublet cannot be described reliably by single-reference methods. Therefore, the transition state was also optimized at the CASPT2 level of theory, which is appropriate for such a situation. We have to describe a reaction and, thus, have to take care that the reactants in the entrance channel are treated in the same way as in the interaction region. This is accomplished by restricting the active space to the absolute minimum necessary. In principle, the interaction of a doublet and a triplet can be treated with three electrons in three active orbitals. In the present case, this choice caused convergence problems, and thus, the active space was extended by two active orbitals and four electrons, which removed the problems. The optimized transition state resembles the MP2 structure fairly closely. The main differences are that the C−H bond is found slightly shorter (1.210 Å), the H···O interaction is somewhat longer (1.556 Å), and the C−H···O angle is a bit more acute (137.4°). Especially the latter two deviations support the suspicion that there is a weak O···O interaction present between the two open-shell fragments. The reason why MP2 works in this case can be readily explained by analysis of the CASSCF and CASPT2 wave functions. The wave function shows significant multireference character, but both of the two main electron configurations have only one unpaired electron. These configurations are the bonding and antibonding combinations of a p-type lone pair on the radical O atom and a C−H σ orbital on the radical with one component of the π_g orbital of the O_2 molecule. The remaining singly occupied orbital is the orthogonal π_g component on O_2 that does not interact with the radical. Due to this special situation, the single and double excitations of standard electron correlation methods can compensate the Hartree−Fock error to a large extent.

The second pathway involves an OH radical abstracting the alcoholic hydrogen from the HO group of HMHP. The transition state for this reaction is shown in Figure 3e. This transition state shows the breaking alcoholic O−H bond elongating to 1.128 Å in the transition state and forming a new OH bond of 1.196 Å in making H_2O. The abstraction of the alcoholic hydrogen leads to the $HOOCH_2O$ radical (Figure 2h). It is interesting to compare the $HOCH_2O$ radical (Figure 2g) with the $HOOCH_2O$ radical. Both are alkoxy radicals with the unpaired electron on the terminal oxygen of the C−O bond. In fact, the C−O radical bond is 1.364 Å for $HOCH_2O$ and 1.361 Å for $HOOCH_2O$, indicating that the bonding is quite similar. Even the C−OH bond in $HOCH_2$ and the C−OOH bond in $HOOCH_2O$ are quite similar (i.e., 1.404 and 1.411 Å, respectively), given the −OH and −OOH group differences. There are two pathways by which the $HOOCH_2O$ radical can decompose unimolecularly.

The first is by C−H bond fission to give HC(O)OOH + H. The transition state for this reaction is shown in Figure 3f. There are many features of this transition state that are similar to the C−H bond fission transition state for the $HOCH_2O$ radical (Figure 3c). For example, the dissociating C−H bond in the $HOOCH_2O$ transition state is 1.491 Å, whereas in the $HOCH_2$ transition, it is 1.459 Å. The $^{\bullet}$OCH angles are similar: 94.5° for $HOOCH_2O$ and 94.6° for $HOCH_2O$. The next unimolecular decomposition route for the $HOOCH_2O$ radical is C−O bond fission to produce the HO_2 radical and CH_2O. This transition state is illustrated in Figure 3g. Like the C−H bond fission transition state, in which the $^{\bullet}$OCH angle for the departing

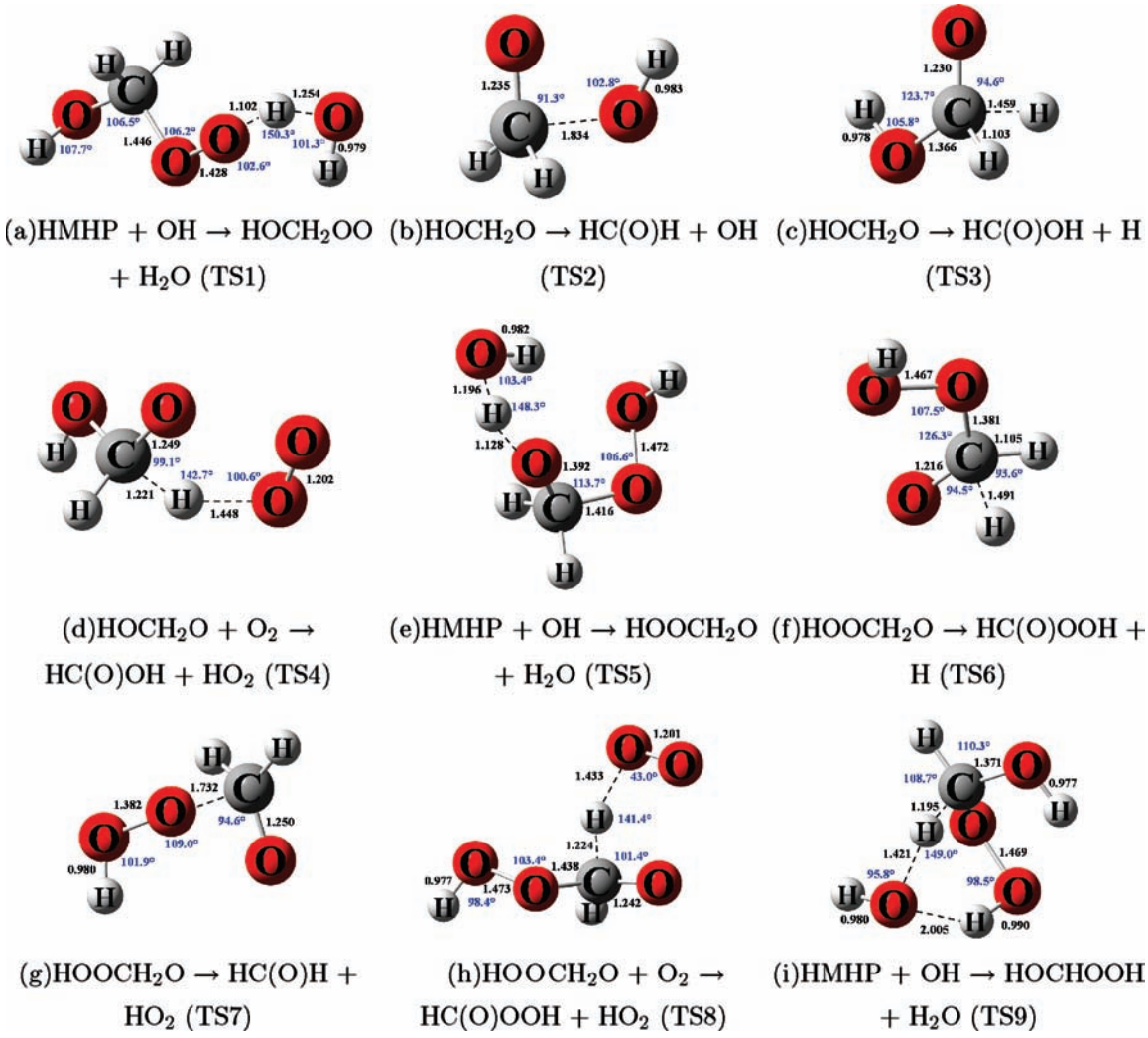

Figure 3. Transition state structures of reactions involved in the atmospheric oxidation of HMHP.

hydrogen atom is 94.5°, the OCO• angle for the departing HO_2 radical is 94.6°. The fragmenting C−O bond is elgonated to 1.732 Å in the transition state. The $HOOCH_2O$ radical can also react with O_2, forming HC(O)OOH and an HO_2 radical (Figure 3h). This reaction causes the C−O• radical bond to shorten to 1.242 Å from 1.361 Å in the $HOOCH_2O$ radical. The abstracted hydrogen from the C−H group increases to 1.224 Å in the transition state, and the H···O−O distance is 1.433 Å. Like TS4 for the reaction of $HOCH_2O$ with O_2, we consider a doublet and a triplet species reacting with each other and, thus, have to account for possible multireference effects. Therefore, we also studied this transition state at CASPT2 level of theory. In this case, it was possible to just treat the three active electrons in three active orbitals. Of course, the perturbational correlation treatment was performed with all valence electrons. The multireference character of the wave function is slightly less pronounced than found for TS4 and shows very little contribution from configurations with three open shells. This indicates that the MP2 and CCSD(T) results should be fairly trustworthy. The optimized CASPT2 structure is similar to the MP2 result. In particular, the terminal oxygen atom of the O_2 fragment seems to align and to interact with the radical O atom. This is also in close resemblance to TS4. The structural parameters differ slightly from the MP2 values and show a longer C···H bond of 1.363 Å and a shorter H···O distance of 1.356 Å. This is also similar to the findings for TS4. As a consequence of the H atom's being farther apart from the carbon center, the HC(O)OOH fragment assumes an almost planar configuration much closer to the final peroxy acid product.

The third pathway involves an OH radical attack at the hydrogen of the α-carbon of HMHP. This transition state is shown in Figure 3i. An interesting feature of this transition state is that the attacking OH radical not only abstracts the hydrogen on the carbon, but also can be stabilized by hydrogen bonding from the neighboring −OOH group. Because of the stabilization of the transition state by the added hydrogen bonding, the transition state takes on a six-membered, ringlike structure. The hydrogen bond between the OH radical and the HOO group, H−O···HOO−, is 2.005 Å and is reminiscent of strong radical molecule hydrogen bonding.[47] The abstraction of the hydrogen from the α-carbon of HMHP generates a radical center on the carbon of the HOCHOOH radical. The MP2 optimized structure is shown in Figure 2i. The radical center produces significant structural changes in the C−O bonds compared to the parent (Figure 2a). Both C−O bonds are shortened. The most dramatically shortened C−O bond is shortened by 0.044 Å, whereas the C−O bond containing the HOO group is shortened by 0.017 Å. The HOCHOOH radical appears to be stabilized by hydrogen bonding forming a five-membered ring indicated by a H···O hydrogen bond length of 2.215 Å.

HOCHOOH could decompose or react in a number of different ways; for example, by addition of O_2 and follow-up reactions. One particularly interesting pathway is the simple bond fission of the O−OH bond, forming formic acid (HC(O)OH)

TABLE I: Heats of Reaction (kcal mol^{-1}) for Reactions Involved in the Atmospheric Degradation of HMHP

	6-31G(d)	6-31++G(2d,2p)		6-311++G(2df,2p)		
reaction	MP2	PMP4	CCSD(T)	PMP4	CCSD(T)	av
		Pathway 1				
$HOCH_2OOH + OH \rightarrow HOCH_2OO + H_2O$	−24.6	−27.6	−28.9	−28.5	−29.9	−29.1
$HOCH_2OO + NO \rightarrow HOCH_2O + NO_2$	−25.9	−24.2	−16.9	−24.1	−17.8	−21.0
$HOCH_2O \rightarrow HC(O)H + OH$	17.5	15.9	17.6	18.0	19.7	18.9
$HOCH_2O \rightarrow HC(O)OH + H$	−16.6	−2.3	−1.0	−3.3	−0.1	−1.7
$HOCH_2O + O_2 \rightarrow HC(O)OH + HO_2$	−41.7	−42.6	−45.2	−44.1	−46.4	−45.3
		Pathway 2				
$HOCH_2OOH + OH \rightarrow HOOCH_2O + H_2O$	−9.0	−11.1	−11.8	−11.3	−12.0	−11.7
$HOOCH_2O \rightarrow HC(O)OOH + H$	−11.4	0.6	3.9	−0.6	2.8	1.1
$HOOCH_2O \rightarrow HC(O)H + HO_2$	−3.9	−4.9	−4.7	−3.7	−3.6	−3.7
$HOOCH_2O + O_2 \rightarrow HC(O)OOH + HO_2$	−36.1	−39.2	−41.5	−32.6	−43.1	−37.9
		Pathway 3				
$HOCH_2OOH + OH \rightarrow [HOCHOOH] + H_2O$	−12.5	−16.0	−15.9	−16.7	−16.6	−16.7
$HOCH_2OOH \rightarrow HC(O)OH + HH_2O$	−71.7	−75.9	−74.5	−75.1	−73.7	−74.4

TABLE II: Barrier Heights (kcal mol^{-1}) for Reactions Involved in the Atmospheric Degradation of HMHP

	6-31G(d)	6-31++G(2d,2p)		6-311++G(2df,2p)		
reaction	MP2	PMP4	CCSD(T)	PMP4	CCSD(T)	av
		Pathway 1				
$HOCH_2OOH + OH \rightarrow HOCH_2OO + H_2O$ (TS1)	12.9	9.4	7.1	2.7	6.4	4.6
$HOCH_2O \rightarrow HC(O)H + OH$ (TS2)	33.4	22.6	25.5	23.4	26.4	24.9
$HOCH_2O \rightarrow HC(O)OH + H$ (TS3)	12.9	10.3	12.5	9.2	11.4	10.3
$HOCH_2O + O_2 \rightarrow HC(O)OH + HO_2$ (TS4)	13.0	6.8	8.5	11.3	6.8	9.1
		Pathway 2				
$HOCH_2OOH + OH \rightarrow HOOCH_2O + H_2O$ (TS5)	6.9	4.7	5.0	3.9	4.2	4.1
$HOOCH_2O \rightarrow HC(O)OOH + H$ (TS6)	20.5	16.5	18.7	15.3	17.4	16.5
$HOOCH_2O \rightarrow HC(O)H + HO_2$ (TS7)	28.1	16.3	17.5	16.4	17.7	17.1
$HOOCH_2O + O_2 \rightarrow HC(O)OOH + HO_2$ (TS8)	13.0	7.5	9.6	5.6	7.9	6.8
		Pathway 3				
$HOCH_2OOH + OH \rightarrow HOCHOOH + H_2O$ (TS9)	5.4	2.0	0.3	1.4	−0.2	0.6

and an OH radical. At first, it seems that this is only one possibility, and we also investigated the O_2 reaction. However, we were unable to locate a transition state for the simple O−OH dissociation reaction on the MP2 surface. A reinvestigation of the problem by CASSCF and CASPT2 methods showed that the intermediate HOCHOOH radical is not a stable species and dissociates spontaneously along the O−OH coordinate. The shallow minimum that we optimized on the MP2 surface is simply an artifact of the single-reference method applied. Due to this spontaneous decomposition, a competing reaction with O_2 is not relevant and is not discussed further.

The dissociation induced by the H abstraction through OH is a rather appealing pathway for two reasons: First, there are no intermediate steps that could pose a bottleneck on the way to the final products. Second and probably more important, the reaction is catalytic in the sense that OH is needed to abstract the H atom, but then another OH is released by the O−OH bond fission so that there is no net consumption of OH radicals. This is potentially of significant relevance in atmospheric chemistry.

2. Energetics of the Species Involved in the Atmospheric Degradation of HMHP. The complete atmospheric degradation mechanism for hydroxy methyl hydroperoxide is shown in Figure 1. The total energies of all species and transition states involved in the present study are given in Tables 3 and 4 of the Supporting Information. Harmonic frequencies and zero-point vibrational energies are reported in Table 5 and 6 of the Supporting Information for reactants and products and transition states, respectively. A list of all the calculated heats of reaction (ΔH_r) as well as reaction barriers (E_a) involved in the mechanism are summarized in Tables I and II.

The energetics diagram for pathway 1 containing the calculated heats of reaction and reaction barriers is shown in Figure 4. The first pathway corresponds to the oxidation process that results from the H abstraction from the peroxy group (−OOH). The hydrogen abstraction by the OH radical requires overcoming an activation barrier of 4.6 kcal mol^{-1}. The transition state corresponds to a first-order saddle point with an imaginary frequency corresponding to the O−H···O vibration at 2903*i* cm^{-1}. In principle, the newly formed peroxy radical, $HOCH_2O_2$ (RI1), could decompose unimolecularly into HC(O)H and HO_2, which, however, turns out to have a much too high barrier (ca. 45 kcal mol^{-1}) to be relevant. By contrast, it can undergo reduction by reaction with NO to produce NO_2 and the $HOCH_2O$ alkoxy radical (RI2).[48] This has a heat of reaction of −21.0 kcal mol^{-1}. It has to be pointed out that the computation of the seemingly simple NO radical leads to problems at the unrestricted open-shell MP2 level. Particularly, the calculated

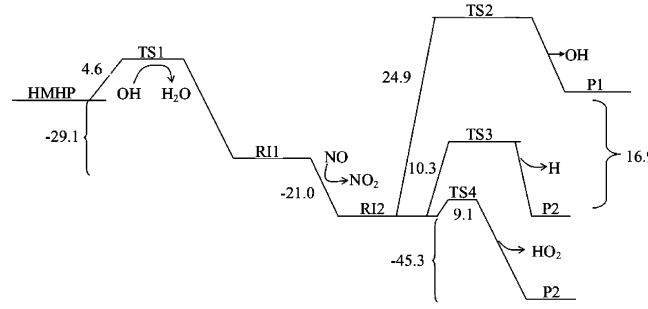

Figure 4. Potential energy profile for the hydrogen abstraction from the −OOH group of HMHP at the CCSD(T)/6-311G(2df,2p)//UMP2/6-31G(d) level of theory (all energies in kcal mol^{-1}).

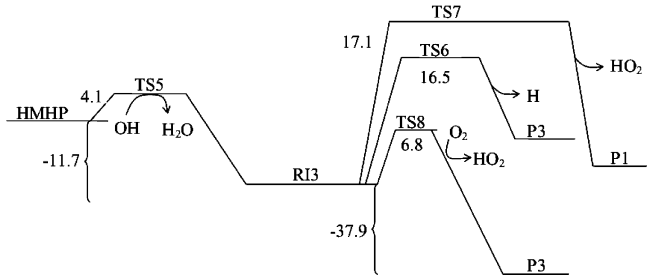

Figure 5. Potential energy profile for the hydrogen abstraction from the C−OH group of HMHP at the CCSD(T)/6-311G(2df,2p)//UMP2/6-31G(d) level of theory (all energies in kcal mol^{-1}).

harmonic frequency is more than twice the correct value. The problem disappears when restricted open-shell MP2 or CCSD(T) is used. This also seems to be the reason for the significant scattering of the reaction heats for reactions that involve NO (Table I.).

The $HOCH_2O$ alkoxy radical can participate in the following reaction pathways:

$$HOCH_2O \rightarrow CH_2O + OH \quad (1)$$

$$HOCH_2O \rightarrow HC(O)OH + H \quad (2)$$

$$HOCH_2O + O_2 \rightarrow HC(O)OH + HO_2 \quad (3)$$

Reaction 1 is a unimolecular bond fission reaction that releases OH radicals. This reaction has a heat of reaction of −18.9 kcal mol^{-1} and a barrier height of 24.9 kcal mol^{-1}. Reaction 2 is another unimolecular reaction that releases H atoms and formic acid. The activation barrier for this process is 10.3 kcal mol^{-1}, and the reaction is more or less thermoneutral. This reaction recently has been studied by Henon et al., and the results are very similar.[49] Particularly, the activation energy is in good agreement with the value of 9.6 kcal mol^{-1} that Henon et al. derived from experimental and RRKM rate data.

Which pathway the reaction course follows in the oxidation process is dependent on the excess energy that remains in the $HOCH_2O$ radical following its production from the $HOCH_2O_2$ + NO reaction. Assuming that the reaction exothermicity energy of −21.0 kcal mol^{-1} for the $HOCH_2O_2$ + NO reaction is equally partitioned between the $HOCH_2O$ and NO_2 radicals and neglecting translational kinetic energy, this suggest that the internal energy in the $HOCH_2O$ radical should be, at most, 10.5 kcal mol^{-1}. This would leave the $HOCH_2O$ radical stable against spontaneous loss of OH or H. However, given the barrier height of only 9.1 kcal mol^{-1} and the abundance of O_2, the reaction of the $HOCH_2O$ radical with O_2 forming HC(O)OH and HO_2 will be an important removal mechanism for $HOCH_2O$ radicals. This reaction is −45.3 kcal mol^{-1} exothermic, and the barrier height is 9.1 kcal mol^{-1} for the α-carbon hydrogen abstraction from $HOCH_2O$ radical by O_2. The transition state for the $HOCH_2O$ + O_2 is a first-order saddle point found with an imaginary frequency of 1693i cm^{-1}. The CASPT2 and MRCI energies for the barrier height are even lower than any MP2 or CCSD(T) value, making this route even more likely. The most reliable value obtained by MRCI is only 3.4 kcal mol^{-1}.

Figure 5 is the energy diagram containing the calculated enthalpies of reaction and activation energies for pathway 2. This second pathway corresponds to the oxidation process that results from the H abstraction from the −OH group of HMHP; namely,

$$HOCH_2OOH + OH \rightarrow HOOCH_2O + H_2O \quad (4)$$

This reaction is 11.7 kcal mol^{-1} exothermic and has an activation energy barrier of 4.1 kcal mol^{-1}. Interestingly, the abstraction of the hydrogen from the HO group is competitive with that from the HOO group on HMHP. The newly formed OCH_2OOH alkoxy radical can undergo unimolecular decomposition by the following pathways:

$$HOOCH_2O \rightarrow HC(O)OOH + H \quad (5)$$

$$HOOCH_2O \rightarrow CH_2O + HO_2 \quad (6)$$

Reaction 5 represents the C−H bond fission reaction, and it has an activation energy of 16.5 kcal mol^{-1}, whereas reaction 6 corresponds to the C−O bond breakage with an activation barrier of 17.1 kcal mol^{-1}. However, it is the reaction of the $HOOCH_2O$ radical with O_2 that is the most energetically favored. Reaction 7, which represents the following process,

$$HOOCH_2O + O_2 \rightarrow HC(O)OOH + HO_2 \quad (7)$$

has an activation energy of 6.8 kcal mol^{-1} and reaction exothermicity of −37.8 kcal mol^{-1}. Multireference effects, which are taken into account by CASPT2 and MRCI calculations, might be important in this reaction. The CASPT2 barrier is significantly higher, but the more reliable MRCI value is found to be in excellent agreement with the above value.

The third pathway corresponds to the oxidation process that results from the H abstraction from the carbon. The calculated barrier height for the abstraction of the hydrogen is predicted to be 0.6 kcal mol^{-1} and is the lowest of all three initial processes. The transition state is characteristized by one imaginary frequency of magnitude 1725i cm^{-1} that corresponds to the breaking of the C−H bond while forming the O−H. Interestingly, energetic ordering for abstraction of hydrogen from HMHP goes as the C−H being most favored over the HO and the HOO group.

As discussed in the previous section, the resulting HOCHOOH radical is only found as a shallow minimum on the single-reference MP2 potential energy surface. It is obvious that formic acid as a final product can be formed by a simple O−OH bond fission. It still seems a little surprising that this dissociation occurs without any barrier. On the MP2 PES, such a barrier obviously must exist, though we were unable to locate it because it must be extremely low. A thorough investigation by CASSCF and CASPT2 clearly shows that the dissociation is barrierless and that the minimum on the MP2 surface is an artifact. This again is one of these three electron processes that apparently require a multireference treatment to rule out spurious results.[35] In the radical, the unpaired electron is located mainly at the C atom, whereas in the products, it will end up in the π orbital of OH, resulting in its $^2\Pi$ ground state. During the bond breaking, the O−OH bond must be cleaved in such a way that the new C−O π bond is formed and the remaining unpaired electron is now located on the OH fragment. It is very likely that along this reaction path, a configuration with three unpaired electrons will contribute significantly, which cannot be treated by the single-reference method. This shortcoming of MP2 may

artificially "glue" the fragments together, resulting in the observed shallow minimum. The driving force for this reaction is quite clear, although maybe surprising. This pathway represents the decomposition of HMHP to formic acid and water in which OH radicals only play the role of a catalyst! The reaction energy of -74.4 kcal mol^{-1} is significant, and the barrier of the initial H abstraction by OH is very low. In effect, this means that this is a highly efficient and much preferred pathway when compared to the other two possibilities. This is in very good agreement with the experimental observations, which find mainly formic acid as a final product.

B. Atmospheric Implications. The atmospheric oxidation mechanism of $HOCH_2OOH$ that results from abstraction of hydrogens from the HO, HOO, and CH groups has been assessed in this work. Abstracting the hydrogen from the α-carbon is considered the most favorable pathway. This is because it has to overcome the smallest activation barrier of the three pathways (only 0.6 kcal mol^{-1}). Our somewhat unusual finding is that this abstraction reaction initiates the spontaneous decomposition of the resulting radical into formic acid, releasing an OH radical. This means that HMHP is decomposed into HC(O)OH and water and that OH is needed only as a catalyst, thus not changing the HO_x concentration under atmospheric conditions. It also suggests that this reaction pathway should be rather efficient, not only due to the very low barrier but also because competing reactions after the initial H abstraction are very unlikely. The catalytic nature of this process is of great significance because as a result, the degradation of HMHP is not limited by the OH abundance, like most other atmospheric reactions with OH. Our results are consistent with the experimental finding of Bauerle and Moortgat,[25] who reported that the major product from the loss of HMHP due to reaction with OH radicals is 95% formic acid. Results of this study suggest that pathway 1, which would be a minor route, will also be a contributing source of formic acid as well as HO_2 radicals. Given the abstraction of the hydrogen of the HOO and HO group is competitive, results from this study suggest that another minor product from the atmospheric oxidation of HMHP by OH radicals should be HC(O)OOH, resulting from pathway 2.

In the literature, it is suggested that the two major removal processes for HMHP are photolysis and removal by reaction with OH radicals. Fry et al.[27] studied the photodissociation of HMHP by OH overtone-induced dissociation. The dissociation results in breaking of the O−O bond in the HOO group of HMHP, giving OH + $HOCH_2O$ radicals. The UV photodissociation experiments of Su et al.[23,24] and Bauerle and Moortgat[25] also suggest that photolysis in the UV results in the radical products OH + $HOCH_2O$. Our recent theoretical study[26] of the excited states of HMHP shows that photodissociation on the low-lying excited states of HMHP results in breaking the O−O bond. The consequence of the oxidation of the $HOCH_2O$ radical is seen in pathway 1. Its major fate is via the reaction with O_2 (reaction 3) to form formic acid and HO_2 radicals. Whether the $HOCH_2O$ radical itself can undergo photodissociation is not yet known. This as well as a determination of the resulting photoproducts is the subject of a further study. Nevertheless, both photolysis and reaction of HMHP with OH radicals lead to the same products (namely, HC(O)OH and HO_2) and suggest that HMHP is a contributing atmospheric source of formic acid. Oxidation by OH is also likely to produce HC(O)OOH to some extent.

Acknowledgment. The authors gratefully acknowledge the support of Purdue University Computing Center for generous computer resources to complete this work. We also thank Patrick Blachly for assistance in preparing the figures. We are very grateful for some comments by the referees, which helped us to find the direct dissociation of pathway 3.

Supporting Information Available: Additional information as noted in text. This material is available free of charge via the Internet at http://pubs.acs.org.

References and Notes

(1) Hellpointner, E.; Gäb, S. *Nature* **1989**, *337*, 631.
(2) Seinfeld, J. H.; Pandis, S. N. *Atmospheric Chemistry and Physics*; John Wiley & Sons: New York, 1998.
(3) Hewitt, C. N.; Kok, G. L. *J. Atmos. Chem.* **1991**, *12*, 181.
(4) Fels, M.; Junkermann, W. *Geophys. Res. Lett.* **1994**, *21*, 341.
(5) Lee, J. H.; Leahy, D. F.; Tang, I. N.; Newman, L. *J. Geophys. Res.* **1993**, *98*, 2911.
(6) Lee, M.; Heikes, B. G.; Jacob, D. J.; Sachse, G.; Anderson, B. *J. Geophys. Res. (Atmos.)* **1997**, *102*, 1301.
(7) Kok, G. L.; McLaren, S. E.; Staffelbach, T. A.; Atmos, J. *Ocean. Technol.* **1995**, *12*, 282.
(8) Tremmel, H. G.; Junkermann, W.; Slemr, F. *J. Geophys. Res. (Atmos.)* **1993**, *98*, 1083.
(9) Jackson, A. V.; Hewitt, C. N. *Atmos. Environ.* **1996**, *30*, 819.
(10) Sauer, F.; Schuster, G.; Schafer, C.; Moortgat, G. K. *Geophys. Res. Lett.* **1996**, *23*, 2605.
(11) Sauer, F.; Limbach, S.; Moortgat, G. K. *Atmos. Environ.* **1997**, *31*, 1173.
(12) Staffelbach, T.; Neftel, A.; Blatter, A.; Gut, A.; Fahrni, M.; Stahelin, J.; Prevot, A.; Hering, A.; Lehning, M.; Neininger, B.; et al. *J. Geophys. Res. (Atmos.)* **1997**, *102*, 23345.
(13) Weinstein-Lloyd, J. B.; Lee, J. H.; Daum, P. H.; Kleinman, L. I.; Nunnermacker, L. J.; Springston, S. R. *J. Geophys. Res. (Atmos.)* **1998**, *103*, 22361.
(14) Moortgat, G. K.; Grossmann, D.; Boddenberg, A.; Dallmann, G.; Ligon, A. P.; Turner, W. V.; Gäb, S.; Slemr, F.; Wieprecht, W.; Acker, K.; et al. *J. Atmos. Chem.* **2002**, *42*, 443.
(15) Grossmann, D.; Moortgat, G. K.; Kibler, M.; Schlomski, S.; Bachmann, K.; Alicke, B.; Geyer, A.; Platt, U.; Hammer, M. U.; Vogel, B.; et al. *J. Geophys. Res. (Atmos.)* **2003**, *108*, 8250.
(16) Francois, S.; Sowka, I.; Monod, A.; Temime-Roussel, B.; Laugier, J. M.; Wortham, H. *Atmos. Res.* **2005**, *74*, 525.
(17) Becker, K. H.; Brockman, K. J.; Bechara, J. *Nature* **1990**, *346*, 256.
(18) Gäb, S.; Hellpointner, E.; Turner, W. V.; Korte, F. *Nature* **1985**, *316*, 535.
(19) Horie, O.; Neeb, P.; Limbach, S.; Moortgat, G. K. *Geophys. Res. Lett.* **1994**, *21*, 1523.
(20) Neeb, P.; Sauer, F.; Horie, O.; Moortgat, G. K. *Atmos. Environ.* **1997**, *31*, 1417.
(21) Sauer, F.; Schafer, C.; Neeb, P.; Horie, O.; Moortgat, G. K. *Atmos. Environ.* **1999**, *33*, 229.
(22) Hasson, A. S.; Orzechowska, G.; Paulson, S. E. *J. Geophys. Res. (Atmos.)* **2001**, *106*, 34131.
(23) Su, F.; Calvert, J. G.; Shaw, J. H. *J. Phys. Chem.* **1979**, *83*, 3185.
(24) Su, F.; Calvert, J. G.; Shaw, J. H.; Niki, H.; Maker, P. D.; Savage, C. M.; Breitenbach, L. D. *Chem. Phys. Lett.* **1979**, *65*, 221.
(25) Bauerle, S.; Moortgat, G. K. *Chem. Phys. Lett.* **1999**, *309*, 43.
(26) Eisfeld, W.; Francisco, J. S. *J. Chem. Phys.* **2008**, *128*, 174304.
(27) Fry, J. L.; Matthews, J.; Lane, J. R.; Roehl, C. M.; Sinha, A.; Kjaergaard, H. G.; Wennberg, P. O. *J. Phys. Chem. A* **2006**, *110*, 7072.
(28) Frisch, M. J.; Trucks, G. W.; Schlegel, H. B.; Scuseria, G. E.; Robb, M. A.; Cheeseman, J. R.; Montgomery, J. A., Jr.; Vreven, T.; Kudin, K. N.; Burant, J. C.; Millam, J. M.; Iyengar, S. S.; Tomasi, J.; Barone, V.; Mennucci, B.; Cossi, M.; Scalmani, G.; Rega, N.; Petersson, G. A.; Nakatsuji, H.; Hada, M.; Ehara, M.; Toyota, K.; Fukuda, R.; Hasegawa, J.; Ishida, M.; Nakajima, T.; Honda, Y.; Kitao, O.; Nakai, H.; Klene, M.; Li, X.; Knox, J. E.; Hratchian, H. P.; Cross, J. B.; Bakken, V.; Adamo, C.; Jaramillo, J.; Gomperts, R.; Stratmann, R. E.; Yazyev, O.; Austin, A. J.; Cammi, R.; Pomelli, C.; Ochterski, J. W.; Ayala, P. Y.; Morokuma, K.; Voth, G. A.; Salvador, P.; Dannenberg, J. J.; Zakrzewski, V. G.; Dapprich, S.; Daniels, A. D.; Strain, M. C.; Farkas, O.; Malick, D. K.; Rabuck, A. D.; Raghavachari, K.; Foresman, J. B.; Ortiz, J. V.; Cui, Q.; Baboul, A. G.; Clifford, S.; Cioslowski, J.; Stefanov, B. B.; Liu, G.; Liashenko, A.; Piskorz, P.; Komaromi, I.; Martin, R. L.; Fox, D. J.; Keith, T.; Al-Laham, M. A.; Peng, C. Y.; Nanayakkara, A.; Challacombe, M.; Gill, P. M. W.; Johnson, B.; Chen, W.; Wong, M. W.; Gonzalez, C.; Pople, J. A. *Gaussian 03, Revision C.02*; Gaussian, Inc.: Wallingford, CT, 2004.
(29) MOLPRO 2006. 1 is a package of ab initio programs written by H.-J. Werner, P. J. Knowles et al.
(30) Møller, C.; Plesset, M. S. *Phys. Rev.* **1934**, *46*, 0618.

(31) Rosado-Reyes, C. M.; Francisco, J. S. *J. Geophys. Res. A* **2007**, *112*, D14310.
(32) Rosado-Reyes, C. M.; Francisco, J. S. *J. Phys. Chem. A* **2006**, *110*, 4419.
(33) Martinez-Aviles, M.; Rosado-Reyes, C. M.; Francisco, J. S. *J. Phys. Chem. A* **2008**, *112*, 7930.
(34) Francisco, J. S. *J. Am. Chem. Soc.* **2003**, *125*, 10475.
(35) Eisfeld, W.; Morokuma, K. *J. Chem. Phys.* **2003**, *119*, 4682.
(36) Werner, H. *Mol. Phys.* **1996**, *89*, 645.
(37) Celani, P.; Werner, H.-J. *J. Chem. Phys.* **2003**, *119*, 5044.
(38) Dunning, T. H., Jr. *J. Chem. Phys.* **1989**, *90*, 1007.
(39) Kendall, R. A.; Dunning, T. H., Jr.; Harrison, R. J. *J. Chem. Phys.* **1992**, *96*, 6769.
(40) Celani, P.; Werner, H.-J. *J. Chem. Phys.* **2000**, *112*, 5546.
(41) Werner, H.-J.; Knowles, P. J. *J. Chem. Phys.* **1988**, *89*, 5803.
(42) Knowles, P. J.; Werner, H.-J. *Chem. Phys. Lett.* **1988**, *145*, 514.
(43) Hoper, U.; Botschwina, P.; Köppel, H. *J. Chem. Phys.* **2000**, *112*, 4132.
(44) Petraco, N. D. K.; Allen, W. D.; Schaefer, H. F. *J. Chem. Phys.* **2002**, *116*, 10229.
(45) Rayez, J. C.; Rayez, M. T.; Halvick, P.; Duguay, B.; Dannenberg, J. J. *Chem. Phys.* **1987**, *118*, 265.
(46) Luo, Q.; Li, Q. S. *J. Phys. Chem. A* **2004**, *108*, 5050.
(47) Hernandez-Soto, H.; Weinhold, F.; Francisco, J. S. *J. Chem. Phys.* **2007**, *127*, 164102.
(48) Sander, S. P.; Friedl, R. R.; Golden, D. M.; Kurylo, M. J.; Huie, R. E.; Orkin, V. L.; Moortgat, G. K.; Ravishankara, A. R.; Kolb, C. E.; Molina, J. J.; et al. Chemical Kinetics and Photochemical Data for Use in Atmospheric Studies, Evaluation Number 14, Jet Propulsion Laboratory, 2003.
(49) Henon, E.; Bohr, F.; Sokolowski-Gomez, N.; Caralp, F. *Phys. Chem. Chem. Phys.* **2003**, *5*, 5431.

JP901735Z